Research Square

Preprints are preliminary reports that have not undergone peer review.
They should not be considered conclusive, used to inform clinical practice,
or referenced by the media as validated information.

Thermal Behavior, Combustion Characteristics, and Physicochemical Properties of Semi-Coke from Oxygen-Limited Fast Pyrolysis of Maikuben Low-Rank Coal

Eldar Kopishev
L. N. Gumilyov Eurasian National University
Ayat Sabitov
sabitov_as_3@enu.kz

L. N. Gumilyov Eurasian National University
Gaini Seitenova
L. N. Gumilyov Eurasian National University
Yelaman Aibuldinov
L. N. Gumilyov Eurasian National University
Gaukhar Tazhkenova
L. N. Gumilyov Eurasian National University
Nurbol Appazov
Korkyt Ata Kyzylorda State University

Research Article

Keywords: Fast pyrolysis, Low-rank coal, Maikuben coal, Semi-coke, Coal tar, SEM/EDS, TG/DSC, GC–MS, Oxygen-limited pyrolysis, Phenolic compounds

Posted Date: May 13th, 2026

DOI: https://doi.org/10.21203/rs.3.rs-9542758/v1

License: This work is licensed under a Creative Commons Attribution 4.0 International License.
Read Full License

Additional Declarations: No competing interests reported.

Version of Record: A version of this preprint was published at Journal of Thermal Analysis and Calorimetry on July 11th, 2026. See the published version at https://doi.org/10.1007/s10973-026-15808-6.

Abstract

The efficient utilization of low-rank coal requires conversion routes that enable both energy recovery and the production of solid and liquid products with practical value. In this study, Maikuben low-rank coal (Pavlodar region, Kazakhstan) was subjected to fast pyrolysis at 600°C under limited air supply (~ 1–2 vol% O_2) with a short vapor residence time of approximately 2 s. The process yielded 43.0 wt% semi-coke, 25.7 wt% liquid products, and 31.3 wt% non-condensable gases. The thermal behavior was examined by TG/DSC, the mineralogical and structural transformations were investigated using XRF, XRD, and FTIR, the surface morphology and local elemental composition were characterized by SEM/EDS, and the liquid fraction was analyzed by GC–MS after solvent extraction. The semi-coke exhibited improved thermo-oxidative stability, enrichment in refractory mineral phases, and reduced contents of volatile inorganic components (S, Cl, K). SEM imaging revealed a transformation from compact coal to porous, honeycomb-like semi-coke, while EDS confirmed surface-level enrichment of Si and depletion of K. The condensable products contained aromatic hydrocarbons, phenolic compounds, oxygenated species, and heterocyclic compounds, with phenolics (phenol, cresols, ethylphenol) representing the dominant identifiable compound class. The combined characterization demonstrates that fast pyrolysis of Maikuben coal is a promising thermochemical route for integrated production of solid and liquid products.

1 Introduction

Coal remains an abundant and strategically important energy resource, particularly in countries with large low-rank coal reserves. However, conventional coal utilization is associated with high CO_2 emissions and the release of SOx, NOx, and particulate matter, which has intensified the search for cleaner thermochemical conversion routes [1, 2].

Among these routes, pyrolysis converts coal into three potentially valuable product streams: a carbon-rich solid residue (semi-coke), condensable liquid products (tar/oil), and non-condensable gases [1–4]. In contrast to direct combustion, pyrolysis enables controlled devolatilization and creates opportunities for integrated utilization of both solid and liquid fractions. This is especially relevant for low-rank coals, whose relatively high volatile-matter content makes them promising feedstocks for liquid-rich conversion processes [2–4].

The distribution and composition of pyrolysis products depend strongly on temperature, heating rate, particle size, and vapor residence time. Fast pyrolysis, characterized by rapid heating and short vapor residence times, generally suppresses secondary cracking and repolymerization of primary vapors, thereby favoring higher tar yields [3–6]. Previous studies have shown that rapid pyrolysis at 500–700°C is particularly effective for maximizing recovery of condensable organics from low-rank coals [5, 6].

Although many coal pyrolysis studies have been carried out under inert atmospheres, oxygen-limited conditions are also of practical interest. A small amount of oxygen can influence devolatilization, heat release, sulfur migration, and the chemistry of oxygen-containing structures without shifting the process

to full combustion [7, 8]. Such conditions may provide partial autothermal support and alter both char properties and tar composition [9, 10].

A limitation of the existing literature is that many studies emphasize only one product stream, and integrated studies that directly relate the properties of the semi-coke to the composition of the liquid fraction under the same conditions remain limited [11–14]. Moreover, morphological characterization of the solid product by SEM/EDS, combined with bulk elemental analysis by XRF, can provide complementary information on the spatial distribution and transformation of mineral matter during pyrolysis.

Therefore, the aim of the present work was to provide an integrated evaluation of the products formed during fast pyrolysis of Maikuben coal at 600°C under limited air supply. The study encompasses product distribution, solid-phase transformations (thermal, mineralogical, structural, and morphological), and the composition of the liquid fraction, in order to assess the technological potential of this process for low-rank coal conversion.

2 Materials and Methods

2.1 Feedstock Characterization

Maikuben coal from the Maikuben basin (Pavlodar region, Kazakhstan) was used as the feedstock. The raw coal was air-dried, crushed, and sieved to obtain a particle size fraction of 0.1–0.2 mm. Proximate analysis was performed according to ASTM D3172 [25] and ultimate analysis according to ASTM D3176 [26]. The results are summarized in Table 1.

Table 1 Proximate and ultimate analyses of raw Maikuben coal

(a) Proximate analysis

Parameter	As-received (wt%)	Dry basis (wt%)
Moisture	12.5	–
Ash	18.7	21.4
Volatile matter	42.3	48.3
Fixed carbon (by diff.)	26.5	30.3

(b) Ultimate analysis (dry basis)

Parameter	wt%
C	52.8
H	3.9
N	0.8
S	1.4
O (by diff.)	19.7
Ash	21.4
HHV (Dulong)	21.1 MJ/kg

The coal is classified as a low-rank brown coal (lignite B) with high volatile matter content (48.3 wt%, dry basis) and moderate ash content (21.4 wt%). The relatively high oxygen content (19.7 wt%) and low calorific value (21.1 MJ/kg) are characteristic of Maikuben basin coals [33]. After drying, a representative sample of 5.00 kg was stored in a desiccator prior to pyrolysis experiments.

2.2 Fast Pyrolysis Reactor

Fast pyrolysis experiments were carried out in a pilot-scale reactor designed for short residence time and limited oxygen availability (Fig. 1). The setup consisted of a horizontal tubular furnace in which the coal sample (5.00 kg) was placed in a stainless steel tray and introduced into the reaction zone [23]. The furnace was preheated to 600 °C before each run.

The reactor was purged with nitrogen at a flow rate of approximately 500 mL/min before pyrolysis. During the process, a controlled residual air flow of 25–50 mL/min was admitted into the reaction zone, corresponding to an oxygen supply of approximately 5–10 mL/min (~1–2 vol% O_2 in the reactor atmosphere). These oxygen-lean conditions ensured primarily pyrolytic decomposition while providing a minor oxidative environment. The coal was rapidly introduced into the hot zone and held at 600 °C with a vapor residence time of approximately 2 s. After this short residence time, the reactor was quickly cooled to stop secondary reactions. Volatile products passed through water-cooled condensers; non-condensable gases were collected in gas bags. Each experiment was performed in batch mode. The char yield was determined gravimetrically, the liquid yield by mass of collected condensate, and the gas yield by difference [24]. All yields are reported on a dry-feed basis. The product yields were reproducible within ±2% absolute error over three repeated runs.

2.3 TG/DSC Analysis

Thermogravimetric analysis combined with differential scanning calorimetry was performed on a Netzsch STA 449 F3 Jupiter instrument. Approximately 5–10 mg of sample was heated from ambient

temperature to 1000 °C at 10 °C/min under air flow (50 mL/min) [29, 30].

2.4 XRF Analysis

Elemental composition of inorganic matter was determined by wavelength-dispersive XRF spectrometry (Bruker S8 Tiger, 4 kW). Ash was prepared by ignition at 750 °C; pressed powder pellets were analyzed for elements from Na to U using calibrated standards [31, 32]. Analyses were performed in duplicate (RSD < 2% for major elements).

2.5 XRD Analysis

Powder XRD was performed on a Bruker D6 Phaser diffractometer (Cu Kα, 40 kV, 15 mA) in the 2θ range 5–80° (step size 0.02°, scan speed 2°/min). Mineral phases were identified using the PDF-2 database [11].

2.6 FTIR Spectroscopy

FTIR spectra were recorded on a Thermo Nicolet spectrometer (4000–400 cm^{-1}, 4 cm^{-1} resolution, 32 scans) using KBr pellets (~1 mg sample in 100 mg KBr) [34]. Spectra were baseline-corrected and normalized to the 1600 cm^{-1} band.

2.7 SEM/EDS Analysis

Surface morphology and local elemental composition were examined using a Hitachi TM4000Plus tabletop SEM (Hitachi High-Tech Corporation, Japan) equipped with a built-in silicon drift detector (SDD) for EDS. Samples were mounted on aluminum stubs using conductive carbon tape and sputter-coated with a thin gold layer (~5–10 nm) to improve surface conductivity. The microscope was operated at 15 kV in backscattered electron (BSE) mode under low-vacuum conditions (~30 Pa). Images were recorded at magnifications from ×500 to ×8000 for the raw coal (working distance ~9.3 mm) and from ×100 to ×8000 for the semi-coke (~9.8 mm). EDS quantification used the standardless ZAF correction method; carbon was excluded due to the carbon tape substrate, and gold was excluded because Au coating was applied to the samples prior to SEM examination.

2.8 GC–MS Analysis

The tarry liquid products were fractionated by sequential solvent extraction: the total liquid was mixed with n-hexane to precipitate asphaltenes, then the hexane-soluble portion was separated on silica gel using n-hexane and 1:1 benzene/ethanol [41, 42]. Each fraction was analyzed by GC–MS on an Agilent

7890B/5977B system with a DB-5ms column (30 m × 0.25 mm × 0.25 μm). Temperature program: 50 °C (2 min hold), 5 °C/min to 300 °C (10 min hold). Helium carrier gas at 1 mL/min; EI mode at 70 eV, m/z 15–500. Compounds were identified using the NIST17 mass spectral library [43]. Chromatographic peaks were integrated using ChemStation autoint1.e; peak areas were normalized to total identified compound area (excluding solvent and system contaminant peaks, primarily polyethylene glycol oligomers) to obtain relative abundance.

3 Results

3.1 Product Distribution

The fast pyrolysis of 5.00 kg of dry Maikuben coal at 600°C (vapor residence time ~ 2 s) produced 2.150 kg of solid semi-coke, 1.285 kg of condensed liquid, and 1.565 kg of non-condensable gases, corresponding to 43.0, 25.7, and 31.3 wt%, respectively (Table 2).

Table 2
Mass balance of fast pyrolysis of Maikuben coal (dry basis)

Feed, g	Semi-coke, g	Liquid, g	Gas (diff.), g	Semi-coke, wt%	Liquid, wt%	Gas, wt%
5000	2150	1285	1565	43.0	25.7	31.3

The liquid yield of 25.7 wt% exceeds values typically reported for tar-rich coals at 600°C (~ 19–20 wt%), suggesting that Maikuben brown coal generates relatively high tar yields favored by the short vapor residence time. The limited oxygen supply (~ 1–2 vol% O_2) did not substantially suppress tar production, indicating that the oxidative influence was minimal and the process conditions closely resembled conventional fast pyrolysis [17].

3.2 TG/DTG/DSC Analysis and Combustion Characteristics

The raw coal underwent multi-stage mass loss when heated in air (Fig. 2), with a total mass loss of 61.6 wt%, leaving ~ 38.4 wt% residue (ash). The DTG curve shows two distinct peaks: −3.33%/min at ~ 301°C (attributed to volatile matter oxidation) and − 4.97%/min at ~ 501°C (char combustion). The DSC signal shows two corresponding exothermic peaks, with the dominant heat release occurring during the char combustion stage (Fig. 3).

The semi-coke shows only 16.9 wt% total mass loss with ~ 83.1 wt% residue. No distinct low-temperature DTG peak is observed; only a single broad event at ~ 454°C (DTG peak rate − 2.41%/min). The absence of a low-temperature peak indicates that virtually all light volatiles had been removed during prior pyrolysis. The semi-coke's DSC profile displays only a single mild exotherm in the 400–500°C range, confirming its substantially improved thermo-oxidative stability [29, 30].

To quantify the differences in combustion behavior, characteristic combustion parameters were derived from the TG/DTG curves following the methodology described by Wang et al. [28] and Zhuikov and

Kieush [29]. The ignition temperature (Ti) was determined by the TG–DTG tangent intersection method, the burnout temperature (Tb) was defined as the temperature at which the DTG signal returns to the baseline, and the peak temperature (Tp) corresponds to the maximum mass-loss rate. On the basis of these parameters, three combustion performance indices were calculated: the comprehensive combustibility index $S = (DTG_{max} \times DTG_{mean}) / (T_i^2 \times T_b)$, the ignition index $C = DTG_{max} / T_i^2$, and the combustion stability index $D = DTG_{max} / (T_i \times T_p \times \Delta T)$, where $\Delta T = T_b - T_i$ [28]. The results are summarized in Table 3.

Table 3
Combustion characteristic parameters of raw coal and semi-coke (10°C/min, air)

Parameter	Raw Coal	Semi-Coke
Ti (°C)	248	387
Tp1 (°C)	301	–
Tp2 / Tp (°C)	501	454
Tb (°C)	582	538
DTGmax (%/min)	4.97	2.41
DTGmean (%/min)	1.43	0.90
Total mass loss (wt%)	61.6	16.9
Residue (wt%)	38.4	83.1
S ($\times 10^{-7}$ %² min^{-2} °C^{-3})	1.98	0.27
C ($\times 10^{-5}$ % min^{-1} °C^{-2})	8.08	1.61
D ($\times 10^{-7}$ % min^{-1} °C^{-3})	1.20	0.91

The ignition temperature of the semi-coke (387°C) is 139°C higher than that of the raw coal (248°C), reflecting the removal of easily oxidizable volatile matter during pyrolysis. The maximum mass-loss rate of the coal (4.97%/min) is 2.1 times that of the semi-coke (2.41%/min), indicating substantially higher reactivity of the parent coal. The comprehensive combustibility index S of the coal (1.98×10^{-7}) is 7.4 times higher than that of the semi-coke (0.27×10^{-7}), quantitatively demonstrating the dramatic reduction in overall combustibility after pyrolysis. Similarly, the ignition index C decreases by a factor of 5.0, confirming that the semi-coke requires significantly more energy to initiate combustion. These results are consistent with literature data for lignite-derived chars, where S indices typically decrease by 5–10× after carbonization [28–30].

3.2.1 Kinetic Analysis (Coats–Redfern Method)

The apparent activation energy (Ea) of the combustion reactions was estimated using the Coats–Redfern integral method for a first-order reaction model (n = 1), which is the most commonly applied single-heating-rate approach for coal and char combustion kinetics [28, 30]. The Coats–Redfern equation is expressed as:

$$\ln[-\ln(1-\alpha) / T^2] = \ln[AR / (\beta Ea)] - Ea / (RT)$$

where α is the conversion degree, T is the absolute temperature (K), β is the heating rate (10°C/min), R is the universal gas constant (8.314 J mol^{-1} K^{-1}), A is the pre-exponential factor, and Ea is the apparent activation energy. A plot of $\ln[-\ln(1-\alpha)/T^2]$ versus 1/T yields a straight line with slope –Ea/R. The combustion of the raw coal was divided into two stages for separate kinetic analysis: Stage I (volatile combustion, 250–370°C) and Stage II (char combustion, 420–570°C). For the semi-coke, a single stage (390–530°C) was used. The results are presented in Table 4.

Table 4
Kinetic parameters from Coats–Redfern analysis (first-order model, 10°C/min, air)

Sample / Stage	T range (°C)	Ea (kJ/mol)	R^2
Coal – Stage I (volatile)	250–370	75.7	0.967
Coal – Stage II (char)	420–570	126.5	0.991
Semi-coke (single stage)	390–530	119.8	0.977

The raw coal shows two distinct kinetic regimes. Stage I (volatile combustion) has a lower activation energy of 75.7 kJ/mol, consistent with the relatively easy oxidation of light volatile species released during initial devolatilization. Stage II (char combustion) requires a significantly higher Ea of 126.5 kJ/mol, reflecting the greater thermal stability of the residual fixed carbon matrix. These values fall within the ranges reported for lignite combustion in air: 40–80 kJ/mol for volatile-stage and 80–160 kJ/mol for char-stage reactions [28, 30].

The semi-coke exhibits a single activation energy of 119.8 kJ/mol, which is comparable to the coal's char combustion stage (126.5 kJ/mol). This similarity is expected because the semi-coke is essentially the equivalent of the coal's fixed-carbon residue after prior devolatilization – it consists mainly of condensed aromatic carbon and mineral matter, the same material that burns during Stage II of the coal's TG combustion. The absence of a low-Ea volatile combustion stage in the semi-coke kinetics provides additional quantitative evidence that fast pyrolysis at 600°C effectively removed practically all volatile matter from the coal.

It should be noted that the Coats–Redfern method at a single heating rate provides only apparent kinetic parameters and cannot resolve possible compensation effects between Ea and A. More rigorous isoconversional methods (Kissinger–Akahira–Sunose, Ozawa–Flynn–Wall) would require TG experiments at multiple heating rates and are recommended for future work. Nevertheless, the present

analysis is sufficient to demonstrate the substantial kinetic differences between the raw coal and its pyrolysis-derived semi-coke, and the obtained Ea values are internally consistent and agree well with published data [28–30].

3.3 XRF Analysis

XRF results (Table 5) show that pyrolysis significantly alters the elemental composition of the residue.

Table 5
Absolute elemental concentrations (wt%) in raw coal and semi-coke (XRF)

Element	Raw Coal (wt%)	Semi-Coke (wt%)
Si	11.37	24.48
Al	4.25	6.81
Fe	3.47	3.32
Ca	1.69	1.25
Mg	0.48	0.43
Ti	0.31	0.33
S	1.31	0.28
Cl	0.12	< 0.01
K	0.32	0.14

Silicon shows the most pronounced increase due to its thermal stability and overall mass reduction. Sulfur decreases from 1.31 to 0.28 wt% (− 4.7×), consistent with volatilization as H_2S and SO_2 during pyrolysis. Chlorine is reduced below the detection limit (< 0.01 wt%). Potassium decreases from 0.32 to 0.14 wt%. Fe, Ca, and Mg are partially retained as oxides; Ti is fully retained. The resulting semi-coke is thus enriched in thermally stable elements and depleted in volatile impurities, representing a lower-sulfur, lower-chlorine solid fuel [31–33].

3.4 XRD Analysis

The raw coal XRD pattern (Fig. 4) exhibits a sharp quartz peak at ~ 26.6° 2θ, a broad disordered carbon hump at 20–30°, and minor clay mineral (kaolinite, illite) peaks at 12–25°. After pyrolysis, the quartz peak sharpens, the pyrite peak near 33° disappears (consistent with decomposition to pyrrhotite at ~ 600°C), and kaolinite reflections vanish due to dehydroxylation. The amorphous carbon band becomes sharper, indicating increased aromatic ordering of the carbon matrix [11, 13].

3.5 FTIR Spectroscopy

The raw coal spectrum (Fig. 5) shows a broad O–H stretch (3200–3700 cm^{-1}), aliphatic C–H stretches at 2920 and 2850 cm^{-1}, aromatic C = C near 1600 cm^{-1}, carbonyl C = O near 1700 cm^{-1}, and C–O stretching at 1200–1000 cm^{-1}. After pyrolysis, the O–H, aliphatic C–H, and C = O bands are greatly attenuated, while the aromatic C = C band persists. Persistent mineral bands (Si–O at ~ 1030 cm^{-1}, Al–O/Si–O at 500–800 cm^{-1}) indicate thermally stable clay phases. These changes reflect dehydroxylation, cracking of alkyl chains, and aromatic condensation [35–40].

3.6 SEM/EDS Analysis

The SEM images of raw coal (Fig. 6) reveal a compact, dense microstructure with irregular blocky morphology. At ×500–×1000, the particles appear as angular fragments with smooth cleavage surfaces and limited porosity. At ×3000–×8000, layered features are observed corresponding to bedding planes. Bright BSE spots correspond to mineral phases (pyrite, clays) with higher average atomic number than the carbonaceous matrix.

The semi-coke (Fig. 7) shows a profoundly altered morphology. At ×100, particles appear larger and more irregular with visible macropores and spongy texture. At ×500–×1000, a well-developed porous structure is evident with numerous open cavities, voids, and channels giving a honeycomb-like appearance. This porosity results from rapid release of volatile matter (H_2O, CO, CO_2, light hydrocarbons) creating internal pressure that ruptured the coal matrix.

At ×3000–×8000, the pore walls appear thin and partially fragmented, indicating extensive bubble nucleation before densification. BSE images reveal bright mineral aggregates on the surface and within pore walls, more concentrated and agglomerated than in raw coal, indicating thermal treatment promoted migration and surface exposure of inorganic matter.

EDS microanalysis was performed on selected areas (Table 6). Carbon was excluded from quantification because the samples were mounted on carbon tape. Au and Nb signals were excluded: gold was applied as a sputter coating to improve surface conductivity prior to SEM examination, and the Nb Lα line (2.166 keV) overlaps with Au Mα (2.123 keV), making them inseparable at the energy resolution of the SDD detector. Consequently, both elements represent artifacts of the sample preparation procedure and were removed from quantification.

Table 6
EDS elemental composition (normalized, wt% and at%) of raw coal and semi-coke surfaces

Element	Coal wt%	Coal at%	Semi-Coke wt%	Semi-Coke at%
O	42.90	60.50	47.23	62.91
Si	22.20	17.83	29.23	22.18
Al	13.51	11.29	9.78	7.72
Ca	6.77	3.81	6.30	3.35
Fe	3.89	1.57	4.79	1.83
K	4.39	2.53	1.01	0.55
Mg	1.35	1.25	1.66	1.46

The EDS data are consistent with XRF trends. Silicon increases from 22.20 to 29.23 wt%, confirming silicate phase concentration. The Si/Al mass ratio shifts from 1.64 to 2.99, indicating increased relative contribution of quartz versus aluminosilicate phases, consistent with XRD-confirmed kaolinite dehydroxylation. Potassium shows the most pronounced decrease (4.39 to 1.01 wt%, ~ 77% loss), consistent with alkali metal volatilization above 500°C. Iron slightly increases (3.89 to 4.79 wt%), reflecting concentration of iron-bearing residues from pyrite decomposition. Ca and Mg remain relatively stable. The agreement between local (EDS) and bulk (XRF) analyses strengthens the conclusion that fast pyrolysis selectively removes volatile inorganic species while concentrating refractory phases.

3.7 GC–MS Analysis of Condensable Products

The GC–MS analysis of the tar fractions revealed a complex mixture of organic compounds. A large number of chromatographic peaks in the high-retention-time region (RT > 19 min) were identified as polyethylene glycol (PEG) oligomers and crown ether derivatives (15-crown-5, 18-crown-6) by the NIST17 library with high match quality (80–96). These compounds, which accounted for 90–99% of total peak area depending on the fraction, are attributed to contamination from laboratory consumables, column bleed, or solvent impurities and are excluded from further discussion. The identifiable coal-derived compounds are discussed below and their normalized relative abundances (recalculated excluding contaminant peaks) are presented in Table 7 and Fig. 8a–c.

Table 7
Major compounds identified in pyrolysis tar extracts by GC–MS (normalized area%)

Compound	RT, min	Class	Qual	Hex %	Benz %	EtOH %	Mean %
4-Ethylphenol	17.5	Phenolic	93	29.7	41.9	49.0	40.2
p-Cresol	17.1	Phenolic	96	19.0	24.5	27.1	23.5
Phenol	16.6	Phenolic	94	11.0	13.6	13.5	12.7
2,4-Dimethylphenol	17.7	Phenolic	42–55	18.7	9.5	–	14.1
Dibenzofuran	18.1	O-heterocycle	46	7.5	–	–	7.5
Naphthalene	15.0	PAH	87–93	2.7	3.0	2.1	2.6
1-Methylnaphthalene	15.8–16.0	PAH	64–94	4.6	4.7	6.2	5.2
1,3-Dimethylnaphthalene	16.5	PAH	95	2.1	–	–	2.1
2,3-Dimethylcyclopentenone	13.1	Ketone	76–81	1.3	1.8	–	1.6
2,3-Dihydro-1H-inden-1-one	16.8	Ketone	86	1.6	–	–	1.6

Phenolic compounds dominate the identifiable fraction in all three solvent extracts, collectively accounting for 60–90% of the normalized coal-derived peak area. 4-Ethylphenol is the single most abundant compound (29.7–49.0% across fractions), followed by p-cresol (19.0–27.1%) and phenol (11.0–13.6%). This phenolic dominance is consistent with the 15–30 wt% phenolic content typical of low-rank coal tars [19, 20, 45].

Polycyclic aromatic hydrocarbons (naphthalene, methylnaphthalenes) constitute a secondary group, with combined normalized abundance of 5–10%. Oxygen-containing heterocycles (dibenzofuran) and carbonyl compounds (cyclopentenones, indanone) are present in minor amounts. The presence of these oxygenated species may partly reflect the intrinsic oxygen functionality of the low-rank coal and the mild oxidative atmosphere.

While the original article described a solvent-dependent partitioning of compound classes (nonpolar aromatics in hexane, phenolics in ethanol), the actual GC–MS data show that phenolic compounds are the dominant identifiable class in all three fractions. The observed variation in relative abundances across solvents is relatively modest, likely because phenols are sufficiently soluble in all three extraction solvents at the concentrations present in coal tar.

4 Discussion

The present results demonstrate that fast pyrolysis under limited air supply (~ 1–2 vol% O_2) provides a technically relevant route for simultaneous production of a carbon-rich solid and a chemically complex liquid fraction from Maikuben low-rank coal.

The mass-balance data indicate that the short vapor residence time (~ 2 s) played a decisive role in preserving condensable products. The relatively high liquid yield (25.7 wt%) reflects both the volatile-rich nature of Maikuben coal (48.3 wt% VM, dry basis) and the kinetic advantage of rapid vapor removal. The gas yield (31.3 wt%) is consistent with partial secondary cracking and with the expected contribution of limited oxidative reactions providing mild autothermal support.

The TG/DTG/DSC data and the derived combustion characteristic parameters quantitatively demonstrate the profound impact of fast pyrolysis on the coal's combustion behavior. The ignition temperature increased from 248 to 387°C, the comprehensive combustibility index S decreased by a factor of 7.4, and the ignition index C decreased by a factor of 5.0. These changes are fully consistent with the removal of easily oxidizable volatile components during pyrolysis. The Coats–Redfern kinetic analysis further elucidated the underlying mechanism: the raw coal exhibits a two-stage combustion kinetics with a lower Ea for volatile oxidation (75.7 kJ/mol) and a higher Ea for char burnout (126.5 kJ/mol), whereas the semi-coke shows only a single kinetic regime with Ea = 119.8 kJ/mol, closely matching the coal's char-stage kinetics. This confirms that the semi-coke is essentially a pre-carbonized fixed-carbon residue. From a practical standpoint, the semi-coke may serve as a lower-sulfur, lower-chlorine carbonaceous fuel or reductant, though its higher ignition temperature and ash content must be accounted for in combustion system design.

The XRF data confirm selective volatilization during pyrolysis: Si and Al concentrate in the semi-coke, while S (− 4.7×), Cl (below detection), and K (− 2.3×) are substantially depleted. This is environmentally favorable because the resulting semi-coke has lower potential for sulfur- and chlorine-related emissions.

The SEM/EDS observations provide both morphological and microchemical confirmation of these transformations. The transition from compact coal to porous, honeycomb-like semi-coke visualizes the rapid devolatilization process. EDS microanalysis quantitatively confirmed elemental redistribution at the particle surface level: Si increased from 22.20 to 29.23 wt%, while K decreased by ~ 77%. These local trends are fully consistent with bulk XRF data, demonstrating that selective volatilization occurs at both bulk and surface levels. The Si/Al ratio increase (1.64 to 2.99) at the surface is consistent with kaolinite-to-metakaolin conversion detected by XRD.

The XRD and FTIR results converge on a consistent picture: conversion at 600°C produces a hydrogen-poor, oxygen-depleted, more aromatic char with mineralogical simplification (loss of pyrite and clay phases) and carbon structural ordering.

The GC–MS results show that phenolic compounds (phenol, cresols, ethylphenol) dominate the identifiable coal-derived fraction of the tar, which is characteristic of low-temperature pyrolysis of oxygen-rich low-rank coals [19, 20]. Minor amounts of PAHs (naphthalene, methylnaphthalenes) and oxygenated heterocycles (dibenzofuran) are also present. These compounds represent potentially valuable chemical intermediates: phenolics are feedstocks for resins, adhesives, and pharmaceuticals, while naphthalene derivatives serve as chemical solvents and precursors.

Several limitations should be acknowledged. First, the gas fraction was determined by difference and not compositionally resolved. Second, the exact role of oxygen in shaping tar composition would require comparison with fully inert conditions. Third, the work was carried out at a single temperature and residence time. Fourth, the GC–MS chromatograms showed extensive PEG contamination (likely from laboratory consumables), which limited the number of coal-derived compounds that could be reliably quantified. Improved sample handling and solvent purification protocols would be beneficial for future work.

5 Conclusions

This study demonstrated that fast pyrolysis of Maikuben low-rank coal at 600°C under limited air supply (~ 1–2 vol% O_2) and short vapor residence time (~ 2 s) is an effective route for obtaining both a carbon-rich semi-coke and a chemically complex condensable liquid fraction.

The combined application of TG/DSC, XRF, XRD, FTIR, SEM/EDS, and GC–MS established the relationship between product distribution, thermal behavior, structural, mineralogical, and morphological transformations in the solid residue, and the composition of the liquid products. The semi-coke exhibited improved thermo-oxidative stability, enrichment in refractory mineral phases (Si, Al, Ti), and substantial reduction of volatile inorganic impurities (S: 1.31 → 0.28 wt%, Cl: below detection, K: 0.32 → 0.14 wt%). SEM revealed a pronounced morphological transformation from compact coal to porous, honeycomb-like semi-coke, while EDS confirmed surface-level Si enrichment and K depletion in agreement with bulk XRF data.

The liquid fraction contained phenolic compounds as the dominant identifiable class (phenol, cresols, ethylphenol), along with PAHs (naphthalene, methylnaphthalenes), oxygenated heterocycles (dibenzofuran), and ketones. These compounds represent potentially useful chemical feedstocks for downstream applications.

Future studies should focus on detailed gas-phase analysis, systematic variation of oxygen availability and residence time, improved sample handling protocols for GC–MS analysis, and assessment of the performance of the obtained semi-coke and liquid fractions in downstream applications.

Declarations

Funding This research has been funded by the Committee of Science of the Ministry of Science and Higher Education of the Republic of Kazakhstan (Grants No. BR24992883).

Conflict of Interest The authors declare no conflict of interest.

Data Availability The data that support the findings of this study are available from the corresponding author upon reasonable request.

Author Contributions Conceptualization, Eldar Kopishev, Gaini Seitenova and Yelaman Aibuldinov; Data curation, Ayat Sabitov and Nurbol Appazov; Formal analysis, Eldar Kopishev, Gaini Seitenova and Ayat Sabitov; Funding acquisition, Gaini Seitenova; Investigation, Ayat Sabitov, Gaukhar Tazhkenova and Nurbol Appazov; Methodology, Eldar Kopishev, Gaini Seitenova and Yelaman Aibuldinov; Project administration, Gaini Seitenova; Resources, Gaini Seitenova and Yelaman Aibuldinov; Software, Nurbol Appazov; Supervision, Eldar Kopishev and Gaini Seitenova; Validation, Ayat Sabitov and Gaukhar Tazhkenova; Visualization, Ayat Sabitov; Writing – original draft, Eldar Kopishev, Gaini Seitenova, Yelaman Aibuldinov, Ayat Sabitov, Gaukhar Tazhkenova and Nurbol Appazov; Writing – review & editing, Eldar Kopishev, Gaini Seitenova, Yelaman Aibuldinov, Ayat Sabitov, Gaukhar Tazhkenova and Nurbol Appazov.

References

1. Ofoe JT, Yusuf M, Ibrahim H (2025) A review on coal pyrolysis and gasification: understanding the chemistries and influence of operating conditions. Clean Energy 9(5):3–21
2. Nie F, Meng T, Zhang Q (2017) Pyrolysis of low-rank coal: from research to practice. In: Pyrolysis. InTech
3. Solomon PR, Fletcher TH, Pugmire RJ (1993) Progress in coal pyrolysis. Fuel 72(5):587–597
4. Solomon PR et al (1986) Very rapid coal pyrolysis. Fuel 65(2):182–194
5. Ko G, Peters W, Howard J (1987) Correlation of tar yields from rapid pyrolysis with coal type and pressure. Fuel 66(8):1118–1122
6. Gibbins-Matham J, Kandiyoti R (1988) Coal pyrolysis yields from fast and slow heating in a wire-mesh apparatus. Energy Fuels 2(4):505–511
7. Ma L et al (2022) Investigation of pyrolysis and mild oxidation characteristics of tar-rich coal. ACS Omega 7:25613–25624
8. Butuzova LF et al (1994) Influence of oxygen on the behaviour of oxygen-containing groups in pyrolysis. Fuel 73(6):945–949
9. Bai Z et al (2012) Effect of low concentration of oxygen on removal of stable sulfur in coal. Energy Sources A 34(5):447–455
10. Li X et al (2010) Pyrolysis and combustion characteristics of Indonesian low-rank coal. Energy Fuels 24(1):160–164

11. Ellison C (2023) Analysis of char structure from pyrolysis/gasification of low and middle rank coals. Dissertation
12. Xu Y et al (2020) Effects of vitrinite on structure and combustion reactivity of pyrolysis chars. ACS Omega 5(28):17314–17323
13. Dun W et al (2013) Investigation of structural characteristics of thermally metamorphosed coal by FTIR and XRD. Energy Fuels 27(10):5823–5830
14. Jiang J et al (2007) GC/MS analysis of coal tar composition. Bull Chem Soc Ethiop 21(2)
15. Du H et al (2025) Recycling waste plastics into hydrogen and CNT composites. Clean Energy 9(5):125–135
16. Lv T et al (2021) Pyrolysis of a typical low-rank coal: CPD model. RSC Adv 11(29):17993–18002
17. Shang J et al (2024) Catalytic fast pyrolysis of tar-rich coal with bauxite residue. ACS Omega 9(25):26911–26921
18. Shomanova ZK et al (2017) Study of metallurgy waste as catalyst phases. News Natl Acad Sci Repub Kazakhstan 6(426):195–200
19. Zhao N et al (2019) Component separation and structure characterization of coal tar. Appl Sci 9(20):4335
20. Kong J et al (2014) Formation of phenols during coal flash pyrolysis. Fuel Process Technol 127:41–46
21. Shi Q et al (2024) Pyrolysis behavior of tar-rich coal: TGA and in-situ FTIR study. Fuel 358:130250
22. He L et al (2025) Mechanism of coal pyrolysis to produce aromatics under H_2 atmosphere. Fuel 393:134130
23. Sabitov A et al (2025) Fast pyrolysis technology with solid heat carrier for MSW processing. Eng Sci
24. Xu T, Zhao X, Li Y (2025) Pyrolysis products of tar-rich coal after cryogenic pretreatment. Processes 13(4):1064
25. ASTM D3172 (2024) Standard practice for proximate analysis of coal and coke. ASTM International
26. ASTM D3176 (2024) Standard practice for ultimate analysis of coal and coke. ASTM International
27. ASTM D3174 (2020) Standard test method for ash in coal and coke. ASTM International
28. Wang H, Zhang Y, Sun J (2021) Thermodynamic characteristics of oxidation and combustion of coal. ACS Omega
29. Zhuikov A, Kieush L (2024) Thermogravimetric analysis of combustion of semi-coke. Fire 7(11):385
30. ASTM D6349 Standard test method for major and minor elements in coal. ASTM International
31. Palmer CA (1989) Determination of major and minor elements in coal ash by XRF. USGS
32. Junussov M, Mustapayeva S (2024) Preliminary XRF analysis of coal ash at five Kazakh mines. Appl Sci 14(22):10586
33. Isah UA et al (2024) Correlations of coal rank with FTIR structural parameters: a review. Infrared Phys Technol 141:105456

34. Wu D et al (2020) Fine characterization of Huainan coal using XRD, FTIR, NMR, SEM, AFM. Molecules 25(11):2661
35. Zhang Y, Zhang J, Shi X (2021) Oxidation characteristics of functional groups in coal. ACS Omega 6(11):7669–7679
36. Li H et al (2022) Spectroscopic (FTIR, NMR) and SEM investigation of coal. Fuel 317:123473
37. Xu T et al (2025) Evolution of functional groups during in-situ pyrolysis. J Energy Inst 123
38. Li J (2024) Spectroscopy characteristics of metamorphic graphite. Front Earth Sci
39. He J (2024) Influence of microwave-assisted $scCO_2$ on coal pore structure. ACS Omega
40. Sun M et al (2015) Controlled separation of low temperature coal tar. Fuel Process Technol 136:41–49
41. Liu S et al (2023) Separation and analysis of fractions in low temperature coal tar. Chin J Chem Eng 58:256–265
42. Wallace WE, Moorthy AS (2023) NIST mass spectrometry data center libraries. J Forensic Sci 68(5):1484–1493
43. Yin N (2023) Analysis of tar and pyrolysis gas from low-rank coal. J Renew Sustain Energy 15(4):43102
44. Yi L (2019) Separation of phenolic compounds from coal tar. ACS Sustain Chem Eng
45. Roy A (2021) Insights from PCA applied to Py-GC/MS characterization of coals. Min Metall Explor

Figures

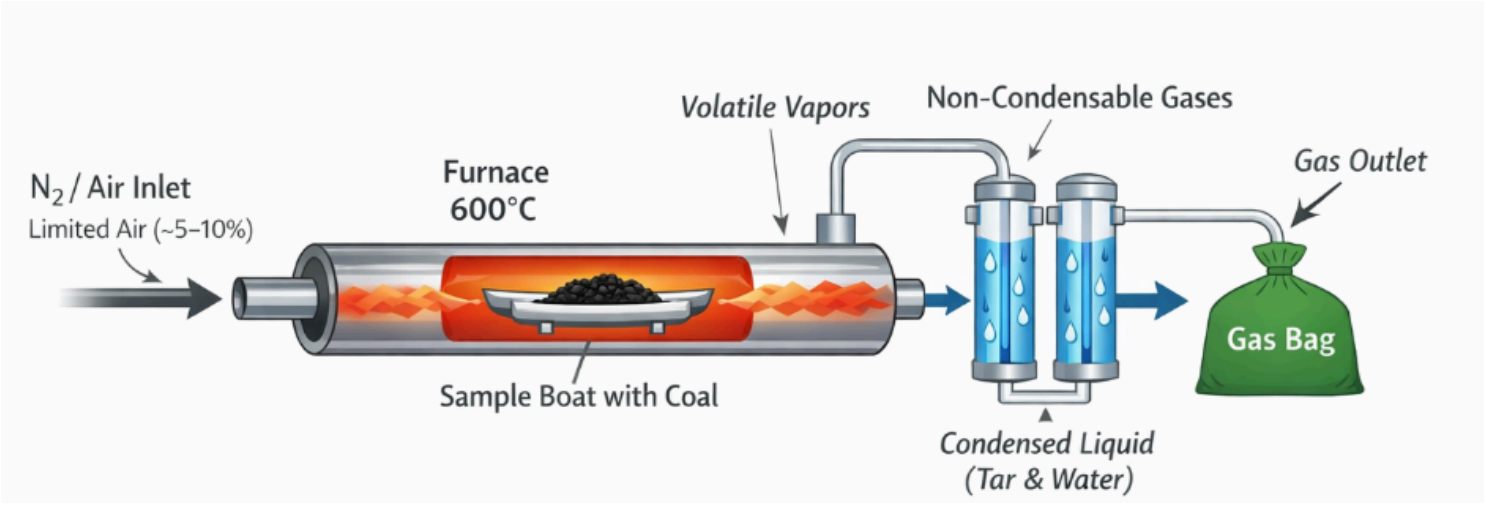


Figure 1

Schematic diagram of the fast pyrolysis reactor setup: (1) nitrogen supply, (2) flow controller, (3) horizontal tubular furnace, (4) stainless steel sample tray, (5) thermocouple, (6) water-cooled condenser train, (7) liquid collection flask, (8) gas sampling bag. The coal sample is rapidly introduced into the pre-

heated reaction zone (600 °C); volatiles pass through condensers where tar is collected, and non-condensable gases are directed to the gas bag.

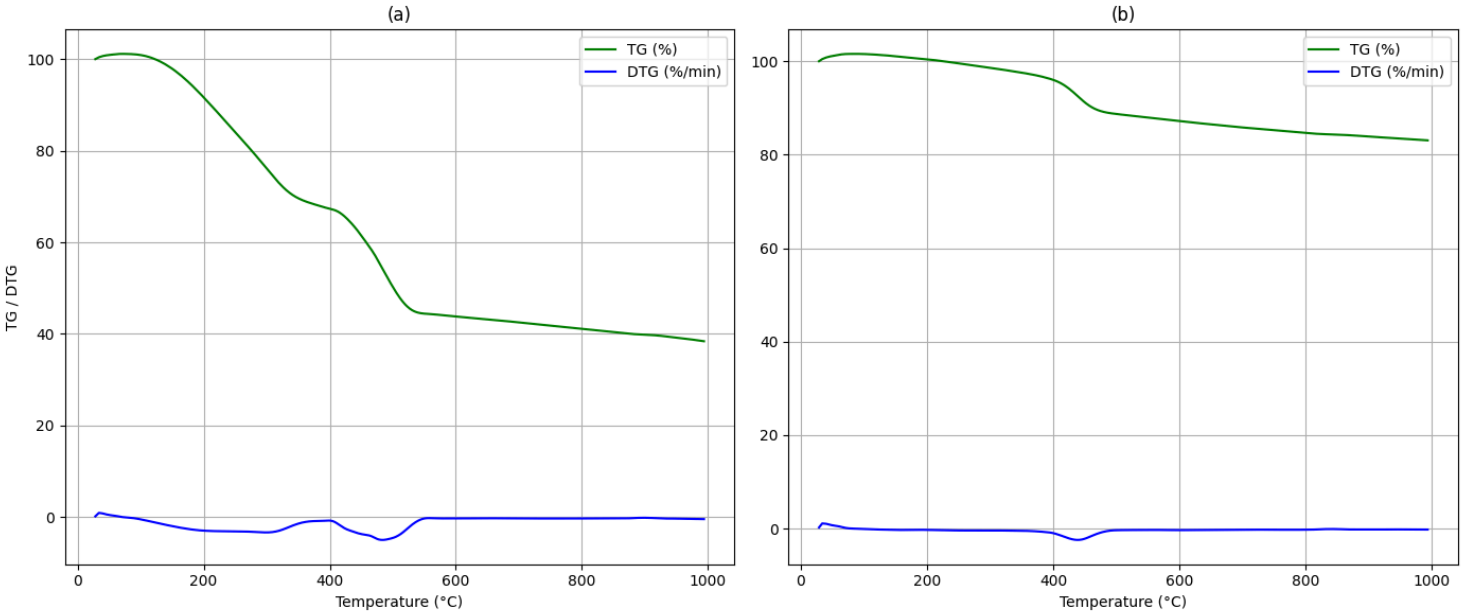


Figure 2

TG and DTG curves for (a) raw Maikuben coal and (b) semi-coke in air atmosphere (heating rate 10 °C/min, air flow 50 mL/min). The coal exhibits two-stage mass loss with DTG peaks at ~301 °C (volatile combustion) and ~501 °C (char burn-off), whereas the semi-coke shows only a single, smaller DTG peak at ~454 °C. Characteristic temperatures Ti, Tp, and Tb are indicated.

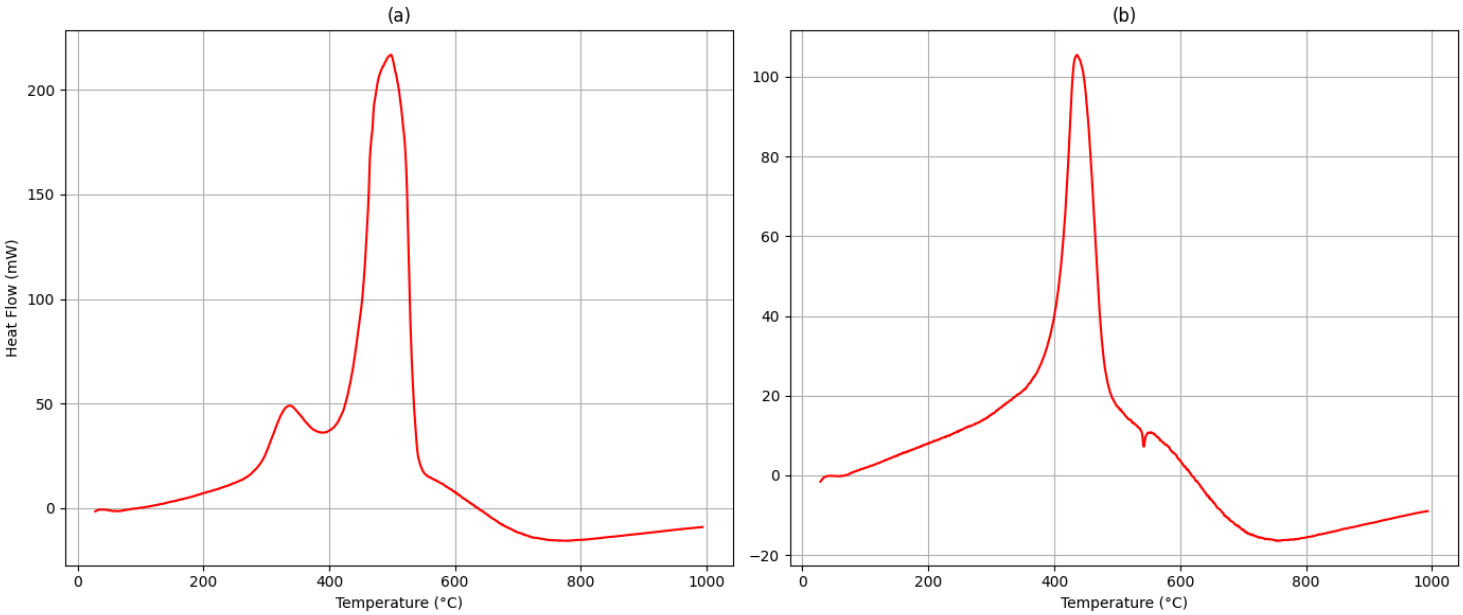


Figure 3

DSC curves for (a) raw coal and (b) semi-coke in air. The coal shows two exothermic peaks corresponding to volatile oxidation (~300 °C) and char combustion (~500 °C). The semi-coke displays only a single broad exotherm at elevated temperature (~450 °C) with markedly lower heat release, confirming improved thermo-oxidative resistance after fast pyrolysis.

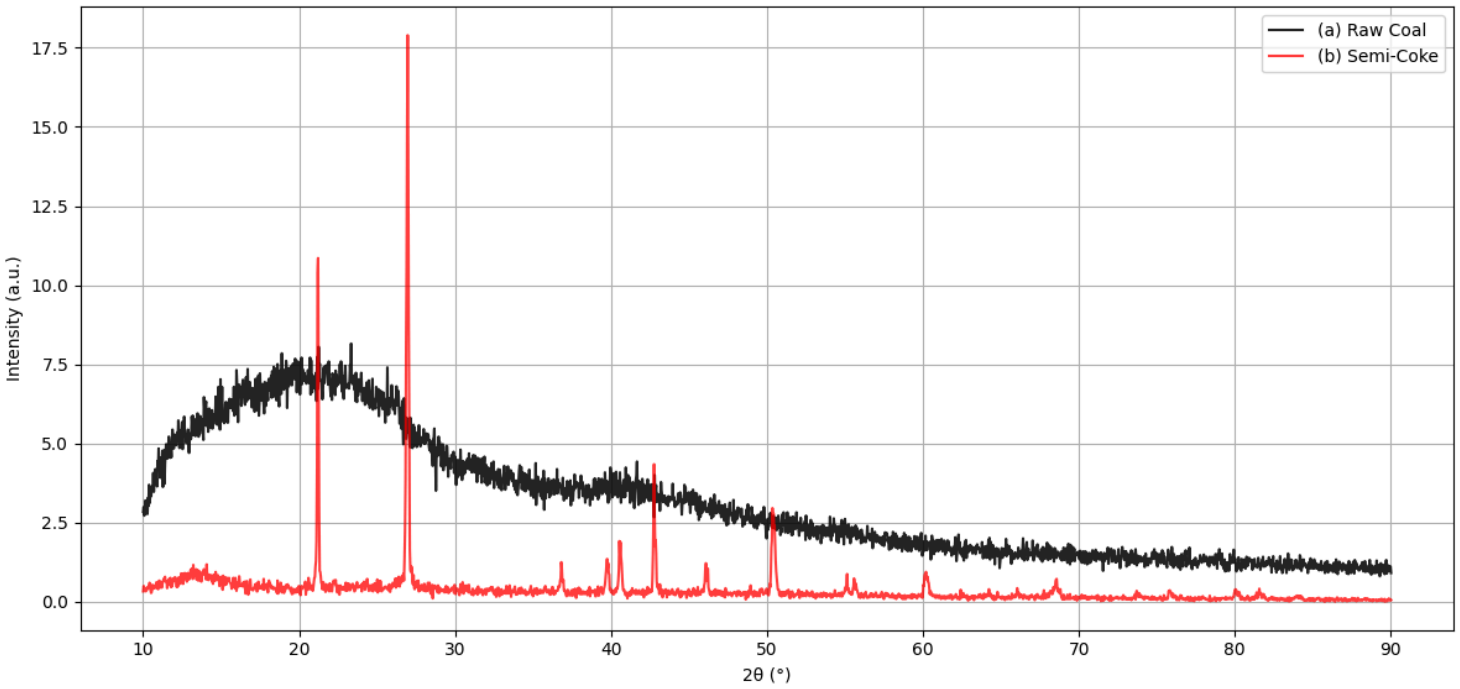


Figure 4

XRD patterns of raw Maikuben coal (bottom) and semi-coke (top). Q – quartz (SiO_2), K – kaolinite, P – pyrite (FeS_2), C – amorphous carbon (002). After pyrolysis, quartz peaks sharpen, pyrite and kaolinite reflections disappear, and the carbon (002) band becomes more defined, indicating progressive aromatic ordering.

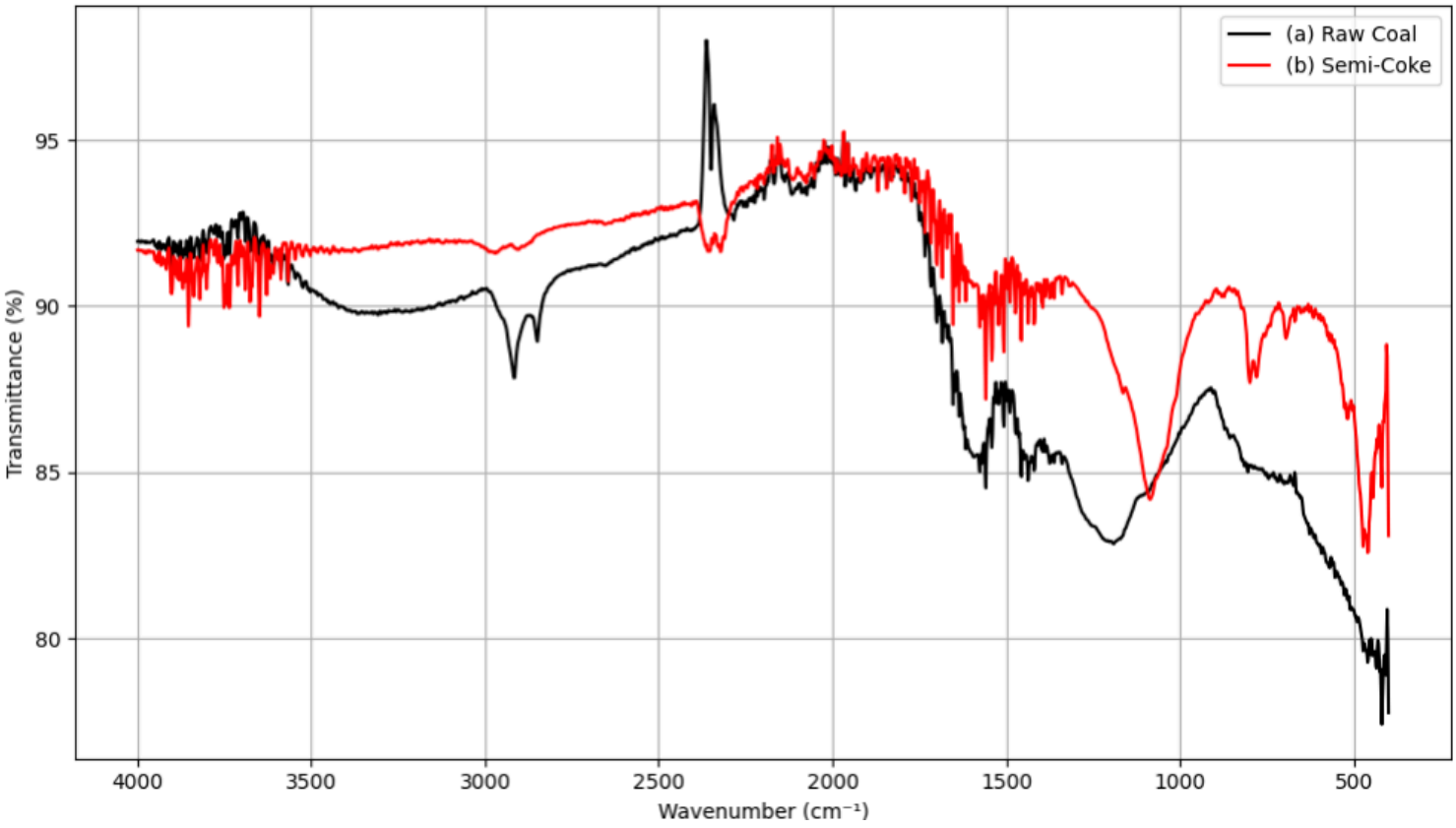


Figure 5

FTIR transmittance spectra of raw coal (bottom) and semi-coke (top) in the 400–4000 cm^{-1} range. Key absorption bands are labeled: O–H (3200–3700 cm^{-1}), aliphatic C–H (2920, 2850 cm^{-1}), C=O (1700 cm^{-1}), aromatic C=C (1600 cm^{-1}), C–O (1000–1200 cm^{-1}), and Si–O (1030 cm^{-1}). The semi-coke shows marked attenuation of O–H, C–H, and C=O bands with retention of aromatic C=C and mineral Si–O features.

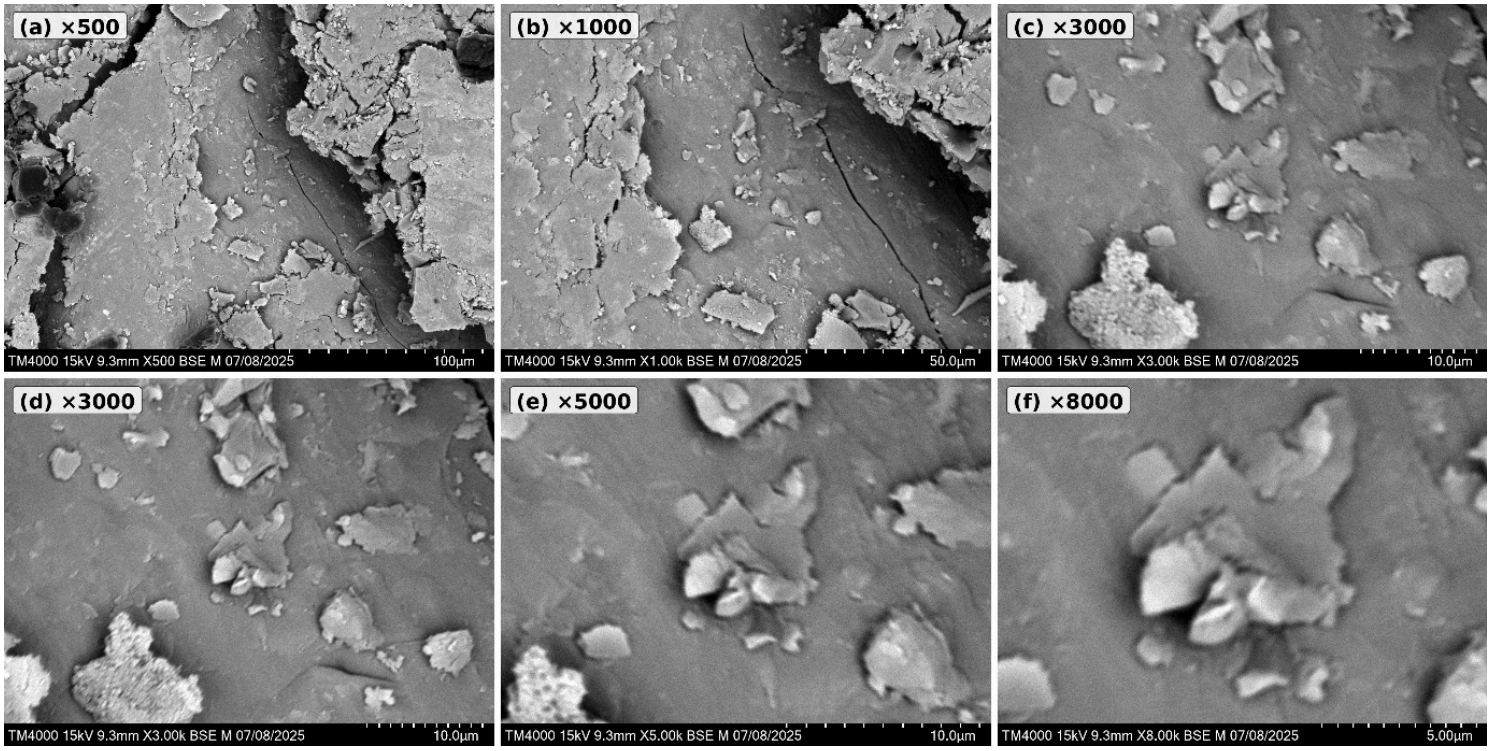


Figure 6

SEM micrographs of raw Maikuben coal at different magnifications: (a) ×500, (b) ×1000, (c, d) ×3000, (e) ×5000, (f) ×8000. BSE mode, 15 kV. The coal exhibits a compact, dense microstructure with angular fragments, smooth cleavage surfaces, and limited porosity. Bright spots correspond to mineral inclusions with higher average atomic number.

Image not available with this version

Figure 7

SEM micrographs of semi-coke after fast pyrolysis at 600 °C: (a) ×100, (b) ×500, (c, d) ×1000, (e, f) ×3000, (g) ×5000, (h) ×8000. BSE mode, 15 kV. The semi-coke displays a well-developed porous, honeycomb-like structure with open voids and channels from rapid devolatilization. Bright mineral aggregates appear concentrated on pore walls.

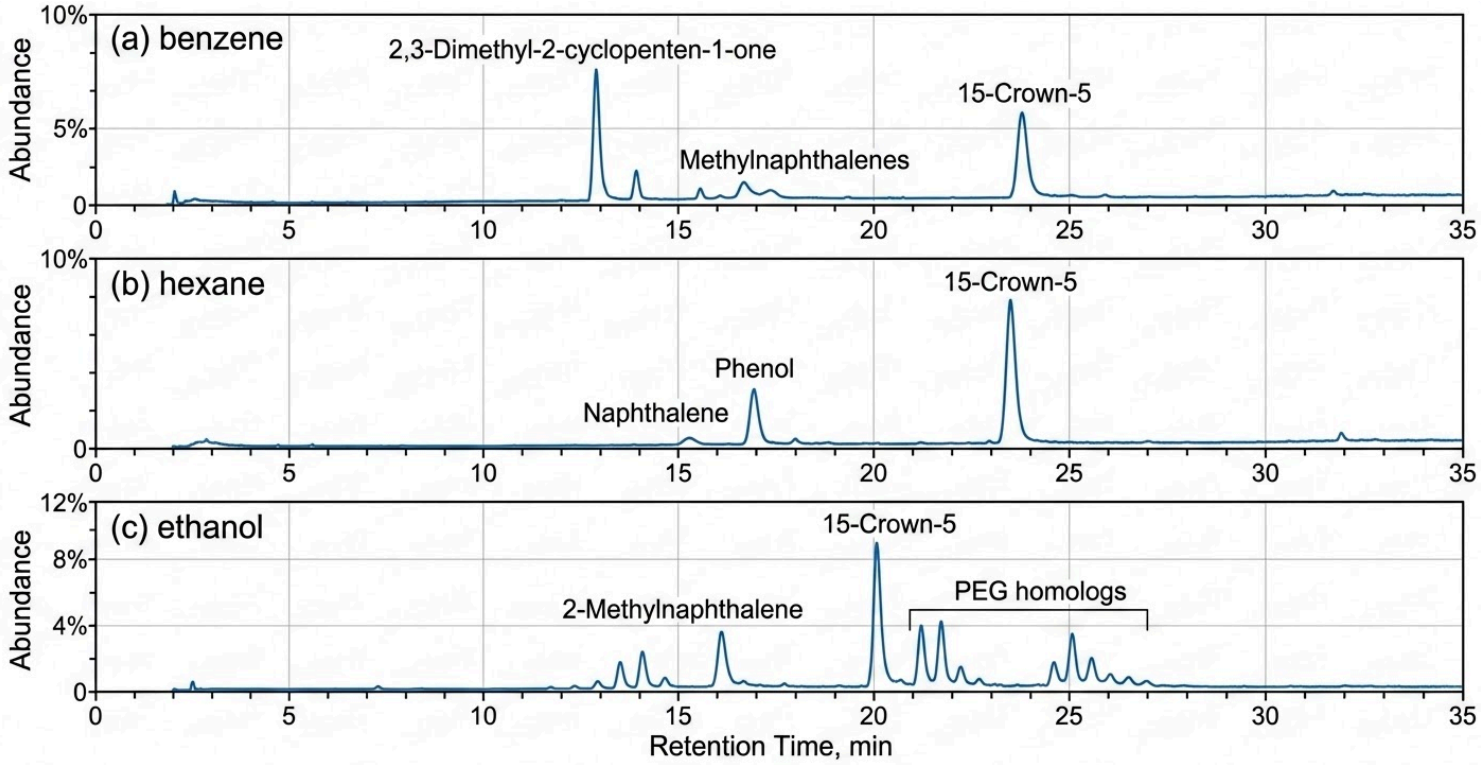


Figure 8

Total ion chromatograms (TIC) of the condensable liquid products extracted with different solvents: (a) hexane extract, (b) benzene extract, (c) ethanol extract. Agilent 7890B/5977B GC–MS, DB-5ms column. Peaks labeled with identified coal-derived compounds; asterisks (*) denote polyethylene glycol contaminant peaks excluded from quantification. The early-eluting region (RT 13–18 min) contains identifiable coal-derived compounds (phenolics, PAHs, ketones), while the later region (RT > 19 min) is dominated by PEG oligomers.